Molecular Crystals and Liquid Crystals Science and Technology. Section A. Molecular Crystals and Liquid Crystals

Publication details, including instructions for authors and subscription information:
http://www.tandfonline.com/loi/gmcl19

Ferromagnetic Spin Alignment in Three-Dimensional Hydrocarbons

Akiomi Mishima [a]

[a] Kanazawa Institute of Technology, Nonoichi, Ishikawa, 921, Japan

Version of record first published: 04 Oct 2006

To cite this article: Akiomi Mishima (1997): Ferromagnetic Spin Alignment in Three-Dimensional Hydrocarbons, Molecular Crystals and Liquid Crystals Science and Technology. Section A. Molecular Crystals and Liquid Crystals, 305:1, 259-268

To link to this article: http://dx.doi.org/10.1080/10587259708045063

Mol. Cryst. Liq. Cryst., 1997, Vol. 305, pp. 259–268
Reprints available directly from the publisher
Photocopying permitted by license only

FERROMAGNETIC SPIN ALIGNMENT IN THREE-DIMENSIONAL HYDROCARBONS

AKIOMI MISHIMA
Kanazawa Institute of Technology, Nonoichi, Ishikawa 921, Japan

Abstract A new three-dimensional (3D) hydrocarbon is proposed as a model of organic ferromagnets. This compound is the 3D-carbon-atom network composed of the benzen rings and the bridging carbon atoms with the itinerant π electrons and the nonbonding electrons. This π-electron system is studied within the Kondo-Hubbard model with the interlayer-transfer energy using a mean-field theory and periodic boundary conditions. The total energy, the energy bands, and the spin densities have been computed. The amplitude of spin density at the bridging carbon atom is most largest. As a result, the spins at the bridging carbon atoms align ferromagnetically in the 3D directions. It turns out that the ferromagnetic ground state is stabilized than the nonmagnetic one through the antiferromagnetic correlation, the ferromagnetic exchange interaction and the topological structure of this compound.

INTRODUCTION

Many researchers have studied progressively organic ferromagnetism for the sake of obtaining organic ferromagnets with high Curie temperatures.[1–3] Hydrocarbons having not d and f electrons but s and p ones have been actively investigated experimentally[4,5] and theoretically.[6,7] Previously, ferromagnetism of a quasi-one-dimensional (Q1D) m-polydiphenylcarbene was proved theoretically by Nasu,[8] and the effects of next-nearest-neighbor transfer integral and nearest-neighbor Coulomb interaction on that were examined by us.[9,10] After that, we pointed out the possibility of ferromagnetism of the 3D-carbon-atom network[11] and then I proposed the Q2D-carbon-atom network occuring ferrromagnetism,[12] because a long-range magnetic order does not appear in strictly 1D and 2D systems.[13]

In this paper, I propose a new 3D hydrocarbon and investigate the electronic and magnetic properties of this compound. It is the 3D-carbon-atom network composed of the benzene rings bridged by the carbon atoms. The π electrons hop between the carbon atoms of the intralayer and between those of two layers, and interact mu-

tually through the antiferromagnetic correlation and further couple ferromagnetically to the localized spin. The Kondo-Hubbard model with the interlayer-transfer energy for this π-electron system is investigated within a mean-field theory with periodic boundary conditions. The total energy per electron, the energy bands, and the spin densities are computed. The purpose of this work is to elucidate that the on-site Coulomb repulsion and the ferromagnetic exchange interaction of the itinerant π electron lead to ferromagnetism due to the topological structure in this compound.

THE KONDO-HUBBARD MODEL

A new hydrocarbon is the 3D-carbon-atom network, as shown in Figure 1. The unit cell is composed of two bridging-carbon atoms (m=1,8), twelve carbon atoms (m=2$\sim$7, 9$\sim$14), and the nonbonding electron with the localized spin (m=0). It is assumed that one π electron per carbon atom moves itinerantly between nearest-neighbor carbon atoms of the intralayer and between those of nearest-neighbor layers. Two π electrons interact antiferromagnetically on the same atom and the spin of the π electron interacts ferromagnetically with the localized spin at the bridging site.

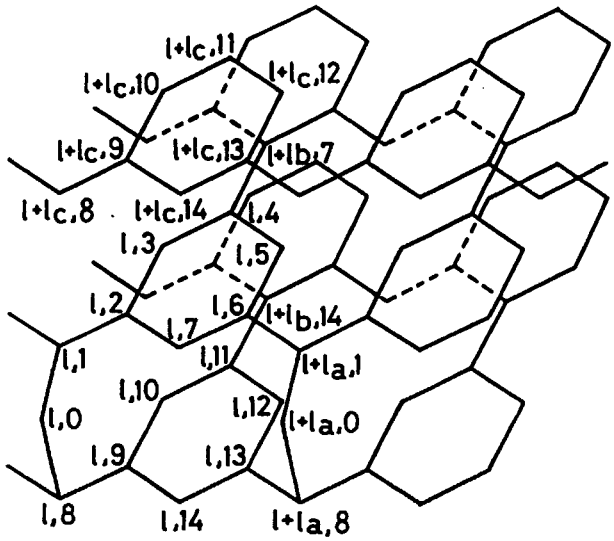

FIGURE 1 Carbon-atom network of the 3D hydrocarbon. The l denotes the l-th unit cell. The m=1$\sim$14 is the carbon-atom site and m=0 is the localized-spin site.

Let us start with the following Hamiltonian :

$$H = H_0 + H_1, \tag{1}$$

where

$$H_0 = -T\sum_{l,\sigma}(\sum_{m=1}^{6} a^{\dagger}_{l,m+1,\sigma}a_{lm\sigma} + a^{\dagger}_{l2\sigma}a_{l7\sigma} + a^{\dagger}_{l+l_b,7,\sigma}a_{l4\sigma} + a^{\dagger}_{l+l_a,1,\sigma}a_{l6\sigma}$$

$$+ \sum_{m=8}^{13} a^{\dagger}_{l,m+1,\sigma}a_{lm\sigma} + a^{\dagger}_{l9\sigma}a_{l14\sigma} + a^{\dagger}_{l+l_b,14,\sigma}a_{l11\sigma} + a^{\dagger}_{l+l_a,8,\sigma}a_{l13\sigma} + \text{H.c.})$$

$$-T_1\sum_{l,\sigma}\sum_{m=1}^{7}(a^{\dagger}_{l,m+7,\sigma}a_{lm\sigma} + a^{\dagger}_{l+l_c,m+7,\sigma}a_{lm\sigma} + \text{H.c.}) \tag{2}$$

and

$$H_1 = U\sum_{l}\sum_{m=1}^{14} n_{lm\alpha}n_{lm\beta} - J\sum_{l}(\mathbf{S}_{l0}\cdot\mathbf{S}_{l1} + \mathbf{S}_{l0}\cdot\mathbf{S}_{l8}), \tag{3}$$

where $a^{\dagger}_{lm\sigma}$ ($a_{lm\sigma}$) denotes the creation (annihilation) operator for the electron of spin σ (σ=α, β, and α and β describe up and down spins, respectively) at site m in the l-th unit cell. The l is l=(n_1, n_2, n_3), where n_1, n_2 and n_3 are arbitrary integers, l_a=$(1,0,0)$, l_b=$(0,1,0)$, l_c=$(0,0,1)$. The $n_{lm\sigma}$=$a^{\dagger}_{lm\sigma}a_{lm\sigma}$ is the number operator. T (T_1) denotes the intralayer- (interlayer-)transfer energy between nearest-neighbor carbon atoms and U denotes the Coulomb repulsive energy of the π electrons on the same carbon atom. $\mathbf{S}_{l1}$ and $\mathbf{S}_{l8}$ are the spin operators of the π electrons at the bridging-carbon-atom sites m=1 and 8 in the the l-th unit cell, respectively. $\mathbf{S}_{l0}$ is the spin operator of the localized spin with the magnitude of spin 1/2 at the site m=0 in the l-th unit cell.

The primitive translation vectors are defined by the equations

$$\mathbf{a} = 2\sqrt{3}\mathbf{x}, \quad \mathbf{b} = 3\mathbf{y}, \quad \mathbf{c} = \mathbf{z}, \tag{4}$$

where $\mathbf{x}$, $\mathbf{y}$ and $\mathbf{z}$ are the Cartesian unit vectors. The lattice vectors become

$$\mathbf{r}_l = n_1\mathbf{a} + n_2\mathbf{b} + n_3\mathbf{c}, \quad \mathbf{r}_{l+l_a} = \mathbf{r}_l + \mathbf{a}, \quad \mathbf{r}_{l+l_b} = \mathbf{r}_l + \mathbf{b}, \quad \mathbf{r}_{l+l_c} = \mathbf{r}_l + \mathbf{c}, \tag{5}$$

and the primitive translation vectors of the reciprocal lattice become

$$\mathbf{A} = \frac{\sqrt{3}\pi}{3}\mathbf{x}, \quad \mathbf{B} = \frac{2\pi}{3}\mathbf{y}, \mathbf{C} = 2\pi\mathbf{z}. \tag{6}$$

The Fourier expansion of the operator $a_{lm\sigma}$ is writtrn as

$$a_{lm\sigma} = \frac{1}{\sqrt{N}} \sum_{\mathbf{k}} \mathrm{e}^{\mathrm{i}\mathbf{k}\cdot\mathbf{r}_l} a_{\mathbf{k}m\sigma}, \tag{7}$$

where N is the total number of unit cell, $\mathbf{k}$ is a wave vector, and the summation over the wave vector is taken under the follwing conditions :

$$0 \leq k_x \leq \frac{\sqrt{3}\pi}{6}, \quad 0 \leq k_y \leq \frac{\pi}{3}, \quad 0 \leq k_z \leq \pi. \tag{8}$$

When the transfer energy T is taken as a unit of energy and the Bloch representation is used, the total Hamiltonian (1) becomes

$$\frac{H}{T} = \frac{H_0}{T} + \frac{H_1}{T}, \tag{9}$$

where

$$\begin{aligned}\frac{H_0}{T} = -\sum_{\mathbf{k},\sigma}\Big(&\sum_{m=1}^{6} a^{\dagger}_{\mathbf{k},m+1,\sigma} a_{\mathbf{k}m\sigma} + a^{\dagger}_{\mathbf{k}2\sigma} a_{\mathbf{k}7\sigma} + \mathrm{e}^{-\mathrm{i}3k_y} a^{\dagger}_{\mathbf{k}7\sigma} a_{\mathbf{k}4\sigma} + \mathrm{e}^{-\mathrm{i}2\sqrt{3}k_z} a^{\dagger}_{\mathbf{k}1\sigma} a_{\mathbf{k}6\sigma} \\ &+ \sum_{m=8}^{13} a^{\dagger}_{\mathbf{k},m+1,\sigma} a_{\mathbf{k}m\sigma} + a^{\dagger}_{\mathbf{k}9\sigma} a_{\mathbf{k}14\sigma} + \mathrm{e}^{-\mathrm{i}3k_y} a^{\dagger}_{\mathbf{k}14\sigma} a_{\mathbf{k}11\sigma} + \mathrm{e}^{-\mathrm{i}2\sqrt{3}k_z} a^{\dagger}_{\mathbf{k}8\sigma} a_{\mathbf{k}13\sigma} + \mathrm{H.c.}\Big) \\ &- \frac{T_1}{T} \sum_{\mathbf{k},\sigma} \sum_{m=1}^{7} (a^{\dagger}_{\mathbf{k},m+7,\sigma} a_{\mathbf{k}m\sigma} + \mathrm{e}^{-\mathrm{i}k_z} a^{\dagger}_{\mathbf{k},m+7,\sigma} a_{\mathbf{k}m\sigma} + \mathrm{H.c.})\end{aligned} \tag{10}$$

with the reations

$$\mathbf{k}\cdot\mathbf{a} = 2\sqrt{3}k_x, \quad \mathbf{k}\cdot\mathbf{b} = 3k_y, \quad \mathbf{k}\cdot\mathbf{c} = k_z. \tag{11}$$

FORMULATION

The mean-field theory is used in order to research the stabilization of the ferromagnetic state for finite U. It is assumed that the system has eight up- and six down-spin π electrons and a localized spin with the magnitude of spin 1/2 in the unit cell.

$$\sum_{m=1}^{14} < n_{lm\alpha} >= 8, \quad \sum_{m=1}^{14} < n_{lm\beta} >= 6, \quad < S^z_{l0} >= 1/2, \tag{12}$$

where $< \cdots >$ denotes the expectation value with respect to the ground state. This state should be determined self-consistently within the mean-field theory. S^z_{l0} is the z component of $\mathbf{S}_{l0}$. The unit of $\hbar = 1$ is used. The neutrality of the carbon atom is also assumed by

$$\sum_{\sigma} < n_{lm\sigma} >= 1 \tag{13}$$

and a half of the spin density is defined by

$$\delta n_m = \frac{1}{2} < n_{lm\alpha} - n_{lm\beta} > . \tag{14}$$

As the Hamiltonians of up- and down-spin electrons are symmetric, the transformations are introduced as follows :

$$a_{lm\alpha} \rightarrow b_{lm\alpha}, a_{lm\beta} \rightarrow (-1)^{m+1} b^{\dagger}_{lm\beta}. \tag{15}$$

The expectation value of Equation (9) becomes

$$< \frac{H}{T} >= \sum_{\mathbf{k},\sigma} \mathbf{b}^{\dagger}_{\mathbf{k}\sigma} M(\mathbf{k}) \mathbf{b}_{\mathbf{k}\sigma} + \frac{NU}{T} \sum_{m=1}^{14} (\delta n_m^2 + \delta n_m) + \frac{N}{2T}(7U + J) \tag{16}$$

with

$$\sum_{m=1}^{14} < b^{\dagger}_{lm\sigma} b_{lm\sigma} >= 8. \tag{17}$$

The $\mathbf{b}^{\dagger}_{\mathbf{k}\sigma}$ is the 14D low vector

$$\mathbf{b}^{\dagger}_{\mathbf{k}\sigma} = [b^{\dagger}_{\mathbf{k}1\sigma}, \cdots, b^{\dagger}_{\mathbf{k}14\sigma}] \tag{18}$$

with the Fourier transform of $b^{\dagger}_{lm\sigma}$,

$$b^{\dagger}_{\mathbf{k}m\sigma} = \frac{1}{\sqrt{N}} \sum_{l} e^{i\mathbf{k}\cdot\mathbf{r}_l} b^{\dagger}_{lm\sigma}. \tag{19}$$

The $M(\mathbf{k})$ is the 14×14 Hermite matrix. Its elements are $M_{m,m}$=$-U\delta n_1/T - J/4T$ (m=1, 8), $M_{m,m}$=$-U\delta n_m/T$ (m=2∼7, 9∼14), $M_{m,m+1}$=$M_{m+1,m}$ =-1 (m=1∼6, 8∼13), $M_{2,7}$=$M_{7,2}$=$M_{9,14}$=$M_{14,9}$= -1, $M_{1,6}$=$M^{*}_{6,1}$=$M_{8,13}$=$M^{*}_{13,8}$= $-\exp(-i2\sqrt{3}k_x)$, $M_{4,7}$=$M^{*}_{7,4}$=$M_{11,14}$= $M^{*}_{14,11}$=$-\exp(-i3k_y)$, $M_{m,m+7}$=$M^{*}_{m+7,m}$= $-1-\exp(-ik_z)$ (m=1, 7) and other elements are 0. By solving the eigenvalue equation

$$M(\mathbf{k})\mathbf{V}_i(\mathbf{k}) = E_i(\mathbf{k})\mathbf{V}_i(\mathbf{k}), \quad (i = 1 \sim 14), \tag{20}$$

the eigenvalue $E_i(\mathbf{k})$ and the eigenvector $\mathbf{V}_i(\mathbf{k})$ of $M(\mathbf{k})$ are got and a half of the spin density is given by

$$\delta n_m = \frac{1}{N} \sum_{\mathbf{k}} \sum_{i=1}^{8} V^{*}_{m,i}(\mathbf{k}) V_{m,i}(\mathbf{k}) - \frac{1}{2}, \tag{21}$$

where the component $V_{m,i}(\mathbf{k})$ of $\mathbf{V}_i(\mathbf{k})$ denotes the amplitude at site m.

RESULTS

From Equation (20), we get fourteen energy bands of the π electrons. They are shown along the k_z axis for U=J=0 and for U/T=1 and J/T=0.5 in Figures 2 and 3, respectively. When U=J=0, the third- and fourth-lowest-energy bands are double in Figure 2. Seven energy bands with negative energies and those with positive ones are symmetric with respect to the Fermi energy E_F. The fifth- and sixth-lowest-energy bands originate from the π electrons at the bridging sites and are twofold degenerate. The degeneracy of the energy band is resolved by finite U and J. The first-, second- and fifth-lowest-energy bands in Figure 2 split into two bands in

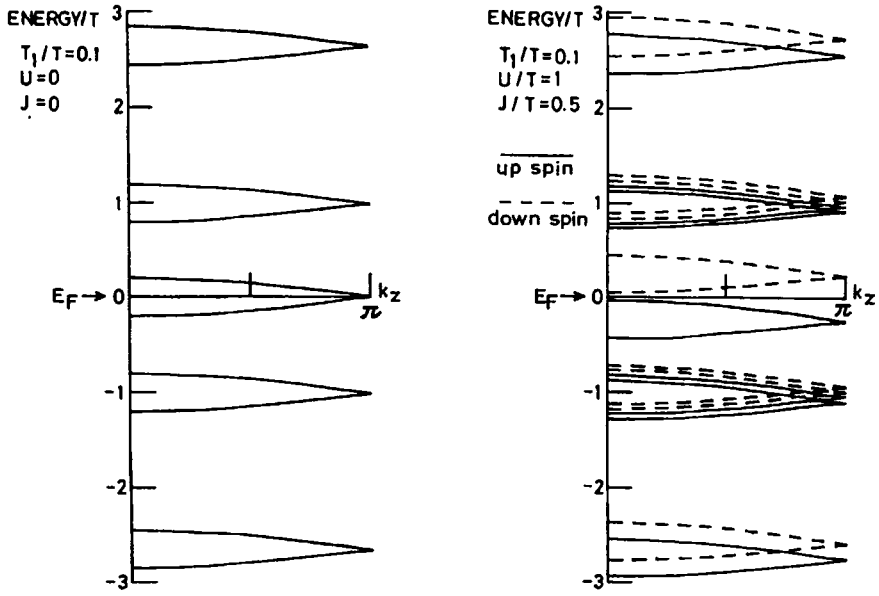

FIGURE 2 Fourteen energy bands of the π electrons along the k_z axis for T_1/T=0.1 and U=J=0. E_F denotes the Fermi energy.

FIGURE 3 Energy bands of the π electrons along the k_z axis for T_1/T=0.1, U/T=1 and J/T=0.5. E_F denotes the Fermi energy. The solid (dashed) lines describe the up- (down-)spin bands.

Figure 3, and the third- and fourth-lowest-energy bands in Figure 2 split into four bands in Figure 3. When U/T=1 and J/T=0.5, the solid and dashed lines indicate the up- and down-spin bands, respectively, in Figure 3. Eight up-spin bands with negative energies and eight down-spin bands with positive ones are symmetric with respect to the Fermi energy E_F, because the up-spin electron and down-spin hole are symmetric. Eight up-spin and six down-spin bands with negative energies are filled by eight up-spin and six down-spin electrons in the ground state, respectively.

Figures 4 and 5 show the energy bands along the k_x and k_y axes for U/T=1 and J/T=0.5, respectively. The energies of the up-spin bands are lower than those of the down-spin ones. Eight up-spin and six down-spin bands from the lowest-energy band are filled by up- and down-spin electrons along the k_x and k_y axes in the ground state, respectively. The seventh- and eighth-lowest-energy bands described by the solid lines are almost flat near the Fermi energy E_F along the k_x and k_y axes, as noticed from Figures 4 and 5. These flat bands originate from the π electrons at the bridging sites. The system has 2^N degenerate ground states and are nonmagnetic for U=J=0. However, a ferromagnetic state can occur, when the bands created by the π electrons at the bridging sites are occupied by the up-spin electrons due to the

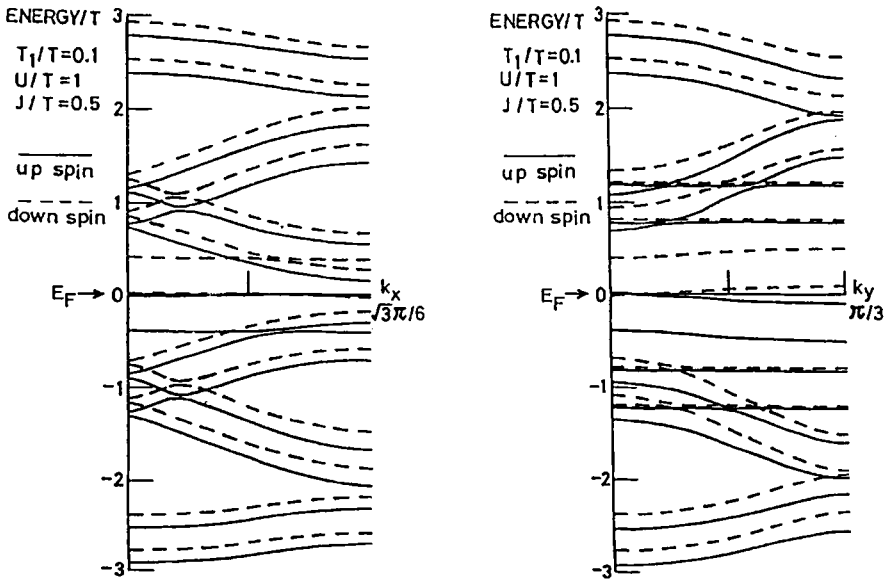

FIGURE 4 Energy bands of the π electrons along the k_x axis.

FIGURE 5 Energy bands of the π electrons along the k_y axis.

topological structure, the ferromagnetic exchange interaction and the Coulomb repulsive one.

From Equations (16) and (20), the total energy per electron in the magnetic state becomes

$$E_{\mathrm{M}} = \frac{1}{7N}\sum_{\mathbf{k}}\sum_{i=1}^{8} E_i(\mathbf{k}) + \frac{U}{14T}\sum_{m=1}^{14}(\delta n_m^2 + \delta n_m) + \frac{1}{4T}(U + \frac{1}{7}J), \tag{22}$$

while the energy per electron in the nonmagnetic state becomes

$$E_{\mathrm{NM}} = \frac{1}{7N}\sum_{\mathbf{k}}\sum_{i=1}^{8} E_{0i}(\mathbf{k}) + \frac{1}{4T}U, \tag{23}$$

where $E_{0i}(\mathbf{k})$ is got from Equation (20) with δn_m=0.

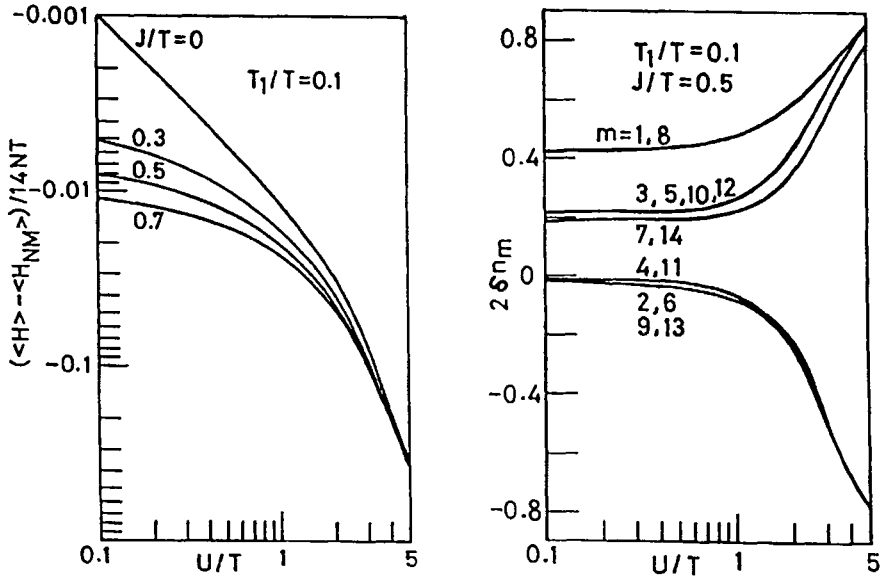

FIGURE 6 Total energy per electron referenced to the nonmagnetic state as a function of U/T for T_1/T=0.1, and J/T=0, 0.3, 0.5 and 0.7.

FIGURE 7 The spin density at site m vs. U/T for T_1/T=0.1 and J/T=0.5.

Figure 6 shows the total energy per electron referenced to the nonmagnetic state as a function of U/T for T_1/T=0.1, and J/T=0, 0.3, 0.5 and 0.7. One sees that the magnetic (spin-density-wave) state is stabilized more by the spin polarization as U/T increases, because the total energy referenced from the nonmagnetic state without spin polarization decreases as U/T increases. As the value of the ferromagnetic exchange interaction J increases from 0, the total energy with negative energy

decreases and thus the ferromagnetic state is more stabilized. As J/T increases from 0 to 0.7, the total magnetic energy per electron referenced to the nonmagnetic state becomes lower for $0.1< U/T <5$. The difference between the magnetic energy for J=0 and that for J/T=0.3, 0.5, or 0.7 becomes smaller with the increase of U/T from 0.1 to 5. Figure 7 depicts the spin density $2\delta n_m$ of the π electron at site m as a function of the on-site Coulomb interaction as a unit of the transfer energy, U/T, for T_1/T=0.1 and $J/T = 0.5$. The amplitudes of the spin densities increase abruptly as U/T increases more than 1, and tend to 1 as U/T goes to infinity. The amplitudes of positive spin densities at the bridging sites m=1 and 8 are most largest, those of positive ones at the benzen-ring sites m=3, 5, 7, 10, 12 and 14 are secondly large, and those of negative ones at the benzen-ring sites m=2, 4, 6, 9, 11 and 13 are most smallest for $0.1< U/T <5$. All spins at the bridging sites become parallel. Therefore, this system has a ferromagnetic (ferrimagnetic)-spin-density distribution.

SUMMARY

I have proposed a new 3D hydrocarbon and sudied the elctronic and magnetic states of the Kondo-Hubbard model with the interlayer transfer and a half-filled band. I have computed the total energy per electron, the energy bands and the spin densities within the mean-field theory using periodic boundary conditions. It has turned out that the antiferromagnetic correlation and the ferromagnetic exchange interaction stabilize a ferromagnetic (ferrimagnetic) state and all spins at the bridging sites align in parallel in this π-electron system with the 3D topological structure.

The Kondo-Hubbard model for the 3D hydrocarbon proposed here has flat bands at the Fermi energy E_F, as shown in Figures 4 and 5, such as the bipartite lattice . The eight sites have positive spin densities and the six sites have negative spin densities due to the antiferromagnetic correlation, as shown in Figure 7. These spin densities at the carbon sites are qualitatively consistent with those of the finite molecule chain by Takui *et al.*'s ENDOR(Electron-Nuclear-Double Resonance) experiment.[14] In this model, the itinerant π electron at the bridging carbon atom couples the localized spin through the ferromagnetic exchange coupling J. As shown in Figure 6, as the value of J increases, the total energy decreases and thus the ferromagnetic state are stabilezed more by J. The amplitude of π-electron spin density is most largest at the bridging carbon atom among the carbon sites for T_1/T=0.1

and $J/T = 0.5$, as shown in Figure 7. All spins at bridging sites become parallel in this π-electron system. Thus the Kondo coupling stabilizes ferromagnetism of the π-electron system in the Kondo-Hubbard model.

Lieb proved rigorously that the ground state has spin $S = ||B| - |A||/2$ ($|B|$ ($|A|$) is the number of sites in the B (A) sublattice) in the repulsive Hubbard model with a half-filled band on a bipartite lattice in all dimensions.[15] He suggested an itinerant-electron ferromagnetism in a periodic lattice with $|B| > |A|$. Recently, it has been showed that the ground states of the Hubbard Hamiltonian for the bipartite inorganic metal-ligand chain and the generaized Hubbard Hamiltonian for the Q1D-organic-bipartite chain have the ferrimagnetic long-range orderings, respectively.[16,17] The 3D structure of the hydrocarbon with the interlayer transfer of the π electron proposed in this paper stabilizes the 3D-long-range order of parallel spins at the bridging carbon atoms. The spin fluctuations have been neglected within the mean-field theory. The effects of spin fluctuations will be studied in future. It is expected that hydrocarbons occuring a ferromagnetic long-range order will be synthesized in future.

REFERENCES

1. O. Kahn, Molecular Magnetism, (VCH, New York, 1993).
2. P.-M. Allemand, K.C. Khemani, A. Koch, F. Wudl, K. Holczer, S. Donovan, G. Grüner, and J.D. Thomson, Science, 253, 301 (1991).
3. M. Takahashi, P. Turek, Y.Nakazawa, M.Tamura, K. Nozawa, D. Shimoi, M. Ishikawa, and M. Kinoshita, Phys. Rev. Lett., 67, 746 (1991).
4. K. Itoh, Chem. Phys. Lett., 1, 235 (1967).
5. H. Iwamura, Pure Appl. Chem., 58, 187 (1986).
6. N. Mataga, Theor. Chim. Acta, 10, 372 (1968).
7. A. A. Ovchinnikov, Theor. Chim. Acta, 47, 297 (1978).
8. K. Nasu, Phys. Rev. B, 33, 330 (1986).
9. A. Mishima and K. Nasu, Synth. Met., 19, 75 (1987).
10. K. Nasu and A. Mishima, Synth. Met., 19, 111 (1987).
11. A. Mishima and K. Nasu, Synth. Met., 22, 23 (1987).
12. A. Mishima, Mol. Cryst. Liq. Cryst., 233, 61 (1993).
13. N. D. Mermin and H. Wagner, Phys. Rev. Lett., 17, 1133 (1966).
14. T. Takui, S. Kita, S. Ichikawa, Y. Teki, T. Kinoshita, and K. Itoh, Mol. Cryst. Liq. Cryst., 176, 67 (1989).
15. E. H. Lieb, Phys. Rev. Lett., 62, 1201 (1989).
16. A.M.S. Macêdo, M.C.dos. Santos, M.D. Coutinho-Filho, and C.A. Macêdo, Phys. Rev. Lett., 74, 1851 (1995).
17. G.S. Tian and T.H. Lin, Phys. Rev. Lett., 534, 8196 (1996).